atmosphere

MDPI

Article

Vertical accelerations and convection initiation in an extreme precipitation event in the western arid areas of Southern Xinjiang

Na Li[1,2,3]*, Lingkun Ran[2]*, Daoyong Yang[4], Baofeng Jiao[5], Cha Yang[4], Wenhao Hu[2], Qilong Sun[6] and Peng Tang[7,]

Supplementary

1.1. Model configurations

The Advanced Weather Research and Forecasting Model (WRF-ARW; version 3.9) was used. The simulation region was shown in Figure 4 which has only one domain, and covered Xinjiang province and its surrounding areas (22.3-49.5°N, 62.7-97°E). The model center was located at 37.1°N, 79.9°E (approximately the rainfall center), with a horizontal grid spacing of 3 km. The number of horizontal grid points was 901×901 in 61 vertical levels from the surface to 50 hPa which had more vertical levels near the surface and the top and fewer middle levels. Rapid Radiative Transfer Model (RRTMG) including the MCICA method of random cloud overlap was used for longwave and shortwave radiation; the planetary boundary layer (PBL) was parameterized by Yonsei University Scheme (YSU) and the Unified Noah land-surface model. The cumulus parameterization scheme was closed and the precipitation was produced by the WRF. Single-Moment 6-class microphysical scheme.

The initial field and lateral boundary conditions are provided by the forecast of the Global Forecasting System (GFS) of National Centers for Environmental Prediction (NCEP) with a horizontal grid spacing of 0.5° and a temporal frequency of 3 h. The experiment was initialized at 0000 UTC on 14 June 2021 and integrated for 48 h. History files were generated in 10min interval. The upper boundary absorbing option damp_opt = 1 was used to avoid any non-physical wave reflection from the top of the model atmosphere

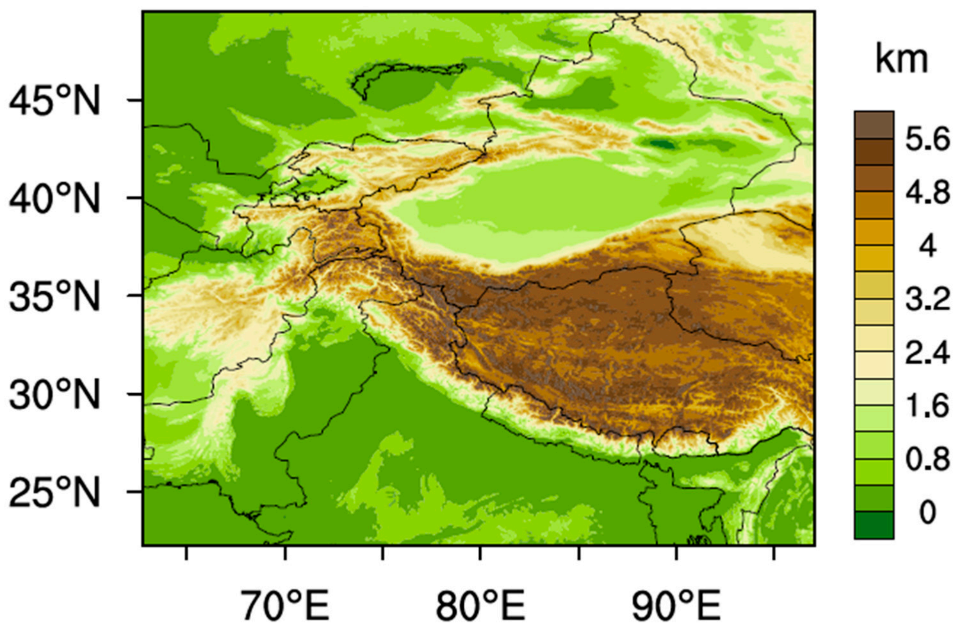

Figure S1. Model domain for the simulation superposed by the terrain height (unit: km).

Figure S2 gives distributions of simulated 6-h precipitation amount during the strong rainfall period at 0600-1800 UTC, June 15, 2021. It shows that the simulation basically reproduces the arc-shaped precipitation pattern from the north slope of Kunlun Mountain northwestward to the concave of Pamir Plateau and then southeastward to the south slope of Tianshan Mountain. Comparing Figs. 5a and 5c, the precipitation in the WRF model appeared to start earlier than the observation, which thus showed larger precipitation during 0600-1200 UTC. The precipitation center in WRF as is enclosed by the blue box, is approximately 50 km wester than the observed extreme precipitation center in CMORPH.

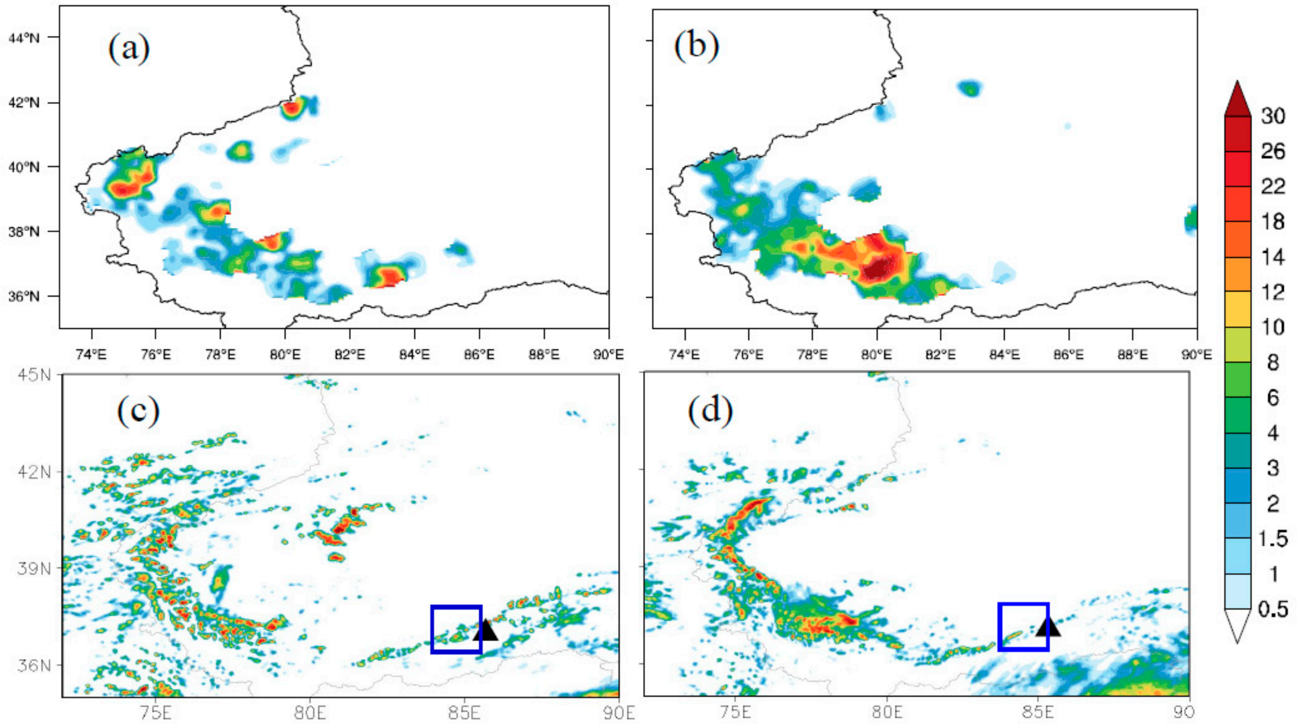

Figure S2. The 6-hr accumulated precipitation from the CMORPH and WRF simulation: **(a, c)** 0600-1200 UTC; **(b, d)** 1200-1800 UTC. The black tringle in Figure 2d marked the observed extreme precipitation center in Figure 2b of CMORPH.

1.2. Comparison of vertical acceleration from different methods

A difference of Net_WAz1 and Net_WAz2 calculated from Equations **Error! Reference source not found.-Error! Reference source not found.**. to Net_WAη which is directly output from the WRF model is shown in supplement files. It verifies that using the WRF output Net_WAη best matches the accelerations within the model. Figure 7. The vertical slices go through the cloud center at 0900 UTC during the initial development of the cumulous. The specific calculation method is introduced in Fig. S3. As is stated above, the vertical acceleration dw/dt, no matter of the calculation methods, should retain unchanged. Figure 7b shows the vertical acceleration dw/dt calculated by with $\partial w/\partial t + \mathbf{v} \cdot \nabla w$. It is characterized by a negative value within the cloud, conforming to the basic distribution of the WRF output Net_WAη (Fig. S3c). Although there is a difference, Figures S3b and S3c at least give evidence on the validity of the WRF output vertical accelerations. In comparison, after remapping the data into the height coordinate, Net_WAz1 and Net_WAz2 largely overestimate the acceleration (one magnitude greater), no matter how the base state is defined, as is shown in Figures S3d-e. It is found that as long as the static balance is satisfied strictly to the base state, Net_WAz1 and Net_WAz2 are basically the same, which means the difference between Figure S3c and Figs. S3d-e is not related to the choice of the base state. The problem is likely caused by the artificially reduction of PGF due to the remapping error. Further, Figure S3f calculate the Net_WAη (not directly output) using basic variables of WRF output in η coordinate without any interpolations. Although there is still a difference with the WRF directly output Net_WAη (Figure S3c) due to some damping procedures before WRF advancing its prognostic variables, the difference is much smaller. Thus, we can believe that WRF-output Net_WAη has maximumly guaranteed the accuracy on the calculation of vertical acceleration. Moreover, considering the independence of dw/dt to the coordinate, we can interpolate Net_WAη into a height coordinate as in Figure S3g, which is basically the same as Fig. S3c for the convenience of analysis.

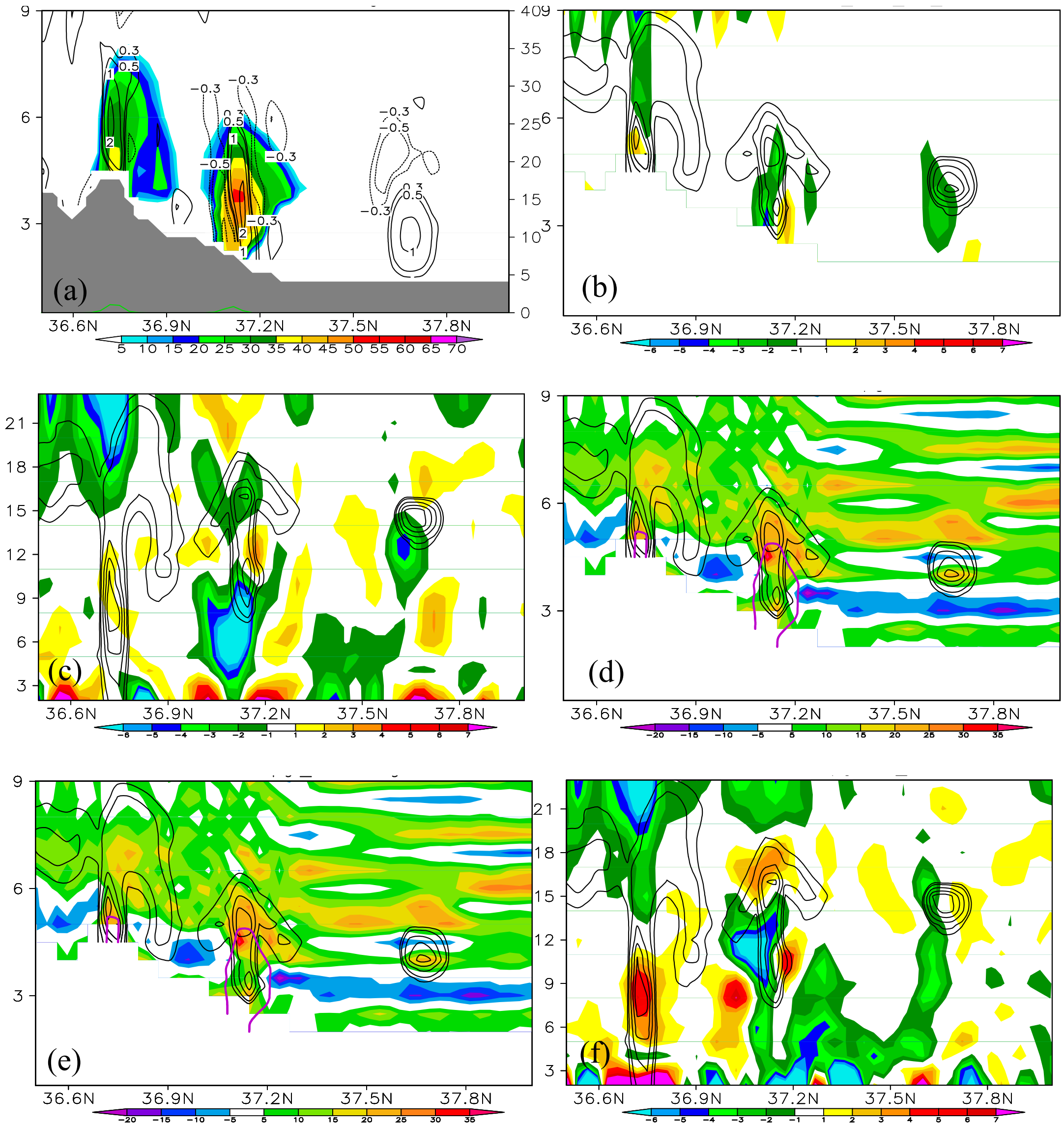

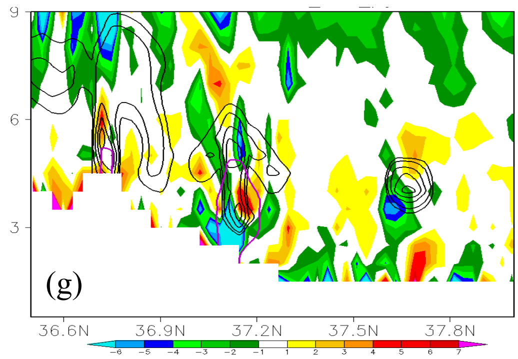

Figure S3. Vertical cross sections of (a) simulated radar reflectivity (shaded, unit: dBz) and vertical velocity (contours, unit: m/s); (b) dw/dt calculated with the left-hand side of Equation (1) in height coordinate, namely $\partial w/\partial t + \mathbf{v} \cdot \nabla w$, in which $\partial w/\partial t$ is calculated with vertical velocity in 10-min interval; (c) WRF output Net_WAη without interpolation to height coordinate; (d) Net_WAη calculated with the right-hand side of Equation (1) using the WRF output fields interpolated to height coordinate; (e) same as (d) but calculated with the right-hand side of Equation (2) with an average over a small-region as the base (34.6-40.6°N, 76-82.9°E); (f) Net_WAη calculated with the WRF output fields in η coordinate with the right-hand terms of Equation (3); (g) same as (c) but interpolated into height coordinate. All the units of (b-g) is 10-3 s-1 and all the pictures are along the cloud core at 78.8°E at 0900 UTC, June 15, 2021. The black contours in (b-g) is mixing ratios of cloud and ice particles (0.05, 0.1, 0.2, 0.3, 0.4 values, unit: g/kg), representing the cloud area. The purple contour in (b-g) is 35-dBz radar reflectivity.